

# Narrowband LTCC Filter with Length-Reduced End-Coupled Resonators

Liangfan Zhu\*

**Abstract**—A narrowband low temperature co-fired ceramic (LTCC) bandpass filter (BPF) with five cascaded physical length-reduced resonators is proposed. Each resonator is built with cascaded horizontal and vertical microstrip lines to produce slow-wave effect, which reduces the physical length of resonators for miniaturization. The entire size of the proposed BPF is only  $15 \times 2 \times 0.3$  mm, and a size reduction of 60% is achieved compared with a traditional implementation. A narrowband fractional bandwidth (FBW) of 4% and an average passband insertion loss of only 2.4 dB are achieved. Comparison and discussion are implemented as well.

## 1. INTRODUCTION

Narrowband bandpass filters (BPFs) have been widely adopted and increasingly required for military phased array radar transceivers. Narrowband BPFs can be constructed with combined structures [1], split ring resonator [2, 3], resistor-loaded resonator [4], cross-coupling structure [5], substrate integrated waveguide [6, 7], open-loop resonator [8], right-left hand resonator [9], and end-coupled resonators [10–12]. Traditional planar end-coupled BPF is constructed with cascaded half-wavelength resonators, and the interconnection between adjacent resonators is via end-coupling effect. However, traditional planar implementation has two problems. First, the length of each resonator is half-wavelength, which results in a large size, especially at low frequencies. Secondly, the coupling gap distance between adjacent resonators is limited less than  $50 \mu\text{m}$  according to printed circuit board (PCB) fabrication process, which is not enough for filter design. BPFs in [8–10] solved the above coupling gap problem by placing resonators on different layers, but helped little for size reduction as the length of resonator was not reduced. BPFs in [13, 14] achieved 80% size reduction using a stacked structure in a low temperature co-fired ceramic (LTCC) substrate. However, BPF in [13] is hard to be mounted or soldered on PCB as its input and output (I/O) ports are installed on the top and bottom sides, respectively. BPF in [14] used a vertical via transition to make I/O ports both on the same side, but the vertical via transition is equal to an inductor, which results in a higher insertion loss.

In this article, a miniaturized and narrowband BPF is proposed and built at a center frequency of 6.5 GHz using a multi-layered LTCC integration process for radar front-end applications. Adopting cascaded slow-wave resonators with cascaded horizontal and vertical microstrip lines and placing resonators on different layers, a size reduction of 60% and a fractional bandwidth (FBW) of 4% are gained compared with a traditional implementation.

---

*Received 18 June 2020, Accepted 4 August 2020, Scheduled 12 August 2020*

\* Corresponding author: Liangfan Zhu (zhuliangfan@hotmail.com).

The author is with the First Business Division Anhui Huadong Photoelectric Technology Research Institute Co., Ltd, Wuhu High and New Technology Industry Development Zone, Anhui, China.

## 2. CIRCUIT DESIGN

### 2.1. BPF Structure Design

Figures 1(a) and (b) show the structure and top geometry view with dimension parameter definitions of the proposed BPF, respectively. For a complete 3D view of the proposed BPF, bottom ground layer is hidden in Figures 1(a) and (b). To make a narrowband and miniaturized BPF at a centre frequency of 6.5 GHz, a multi-resonator structure with cascaded arrangement is selected. The proposed BPF consists of 5-stage half-wavelength resonators, which are buried in a 3-layer LTCC substrate. Resonators 1 and 5 are placed on Layer 1, Resonators 2 and 4 placed on Layer 2, and Resonator 3 placed on Layer 3. The I/O ports are located at Resonators 1 and 5, respectively. Schematic diagram of the proposed BPF is shown in Figure 2. The electrical length of each resonator is half-wavelength based on 6.5 GHz frequency, and the characteristic impedance of each resonator is  $50\ \Omega$ . The broadside coupling effect between neighbouring resonators is controlled by the overlapped area. Weaker coupling effect between resonators and the narrower bandwidth characteristic can be obtained. The arrangement of placing adjacent resonators on different layers solves the minimal gap distance ( $50\ \mu\text{m}$ ) problem of planar implementation. Figure 2 shows the schematic diagram of the proposed BPF. In Figure 2,  $C_{12}$  is the capacitance between Resonators 1 and 2,  $C_{23}$  the capacitance between Resonators 2 and 3,  $C_{34}$  the capacitance between Resonators 3 and 4, and  $C_{45}$  the capacitance between Resonators 4 and 5.

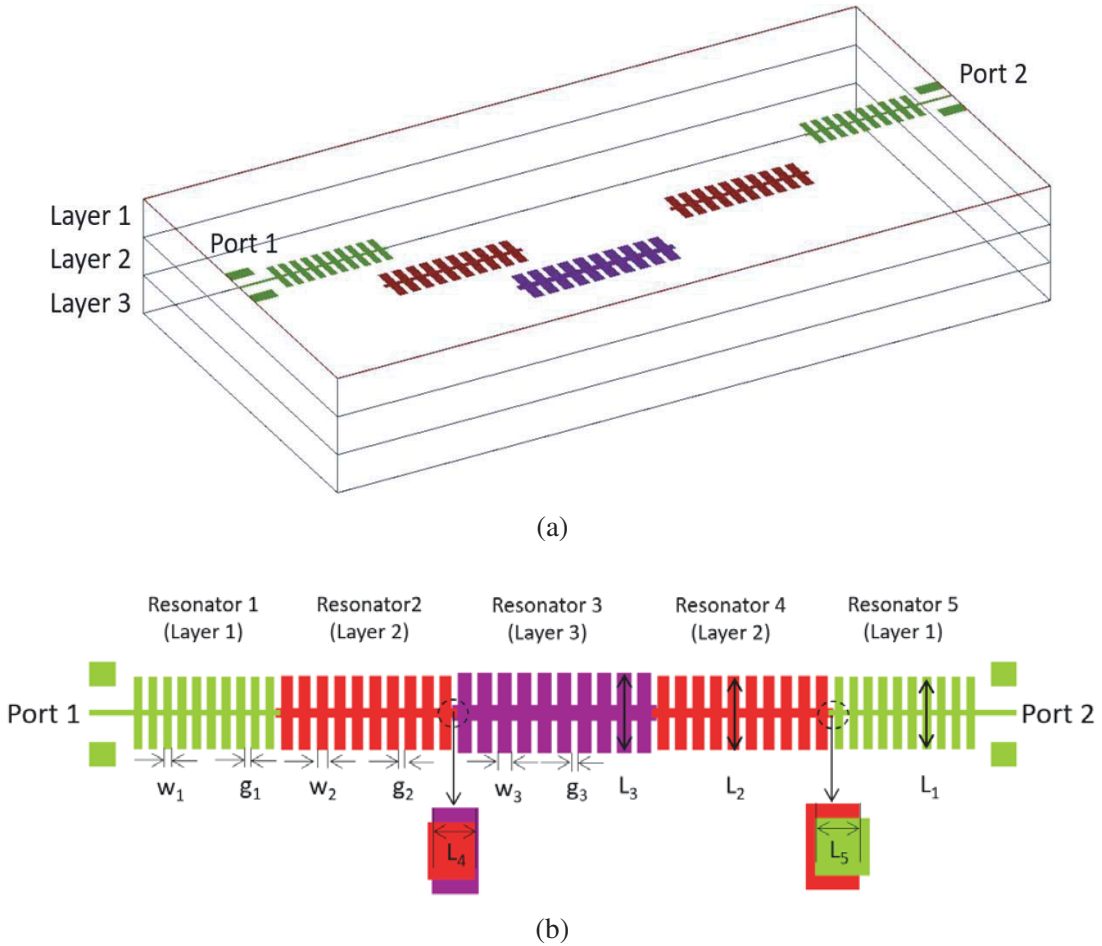


**Figure 1.** The proposed BPF. (a) Structure with bottom ground metal is hidden and (b) top geometry view with dimension parameter definitions.

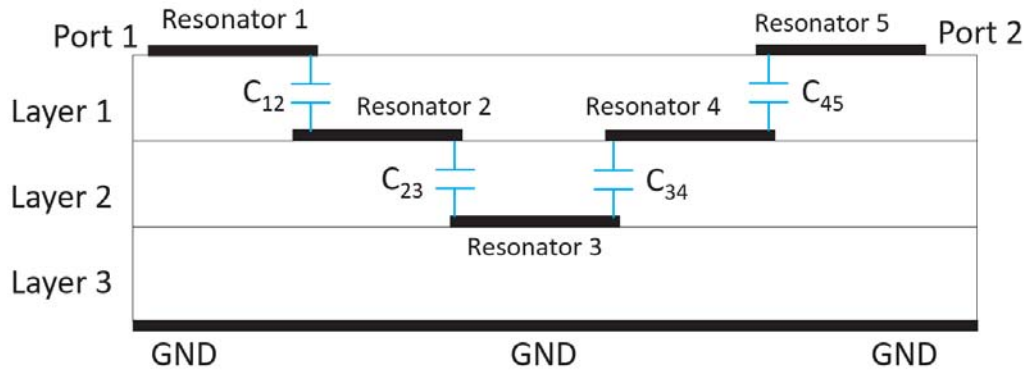


Figure 2. Schematic diagram of the proposed BPF.

### 2.2. Slow-Wave Resonator Design

As each resonator is half-wavelength long, slow-wave structure in Figure 3(a) is used to reduce the physical length of each resonator. Figure 3(b) shows the equivalent circuit of resonators. The horizontal and vertical microstrip lines are equivalent to inductor and capacitor, respectively. The slow-wave structure is constructed by cascaded inductance and capacitance elements. Decreasing the width of horizontal line is to obtain inductance whereas increasing the width of vertical line is to obtain capacitance. The length of half-wavelength resonator can be reduced using the slow-wave structure. For a given transmission line, the ideal characteristic impedance  $Z$  and phase velocity  $V_p$  are well known

$$Z_0 = \sqrt{\frac{L}{C}} \tag{1}$$

$$\lambda = \frac{v_p}{f} \tag{2}$$

$$v_p = \frac{1}{\sqrt{LC}} \tag{3}$$

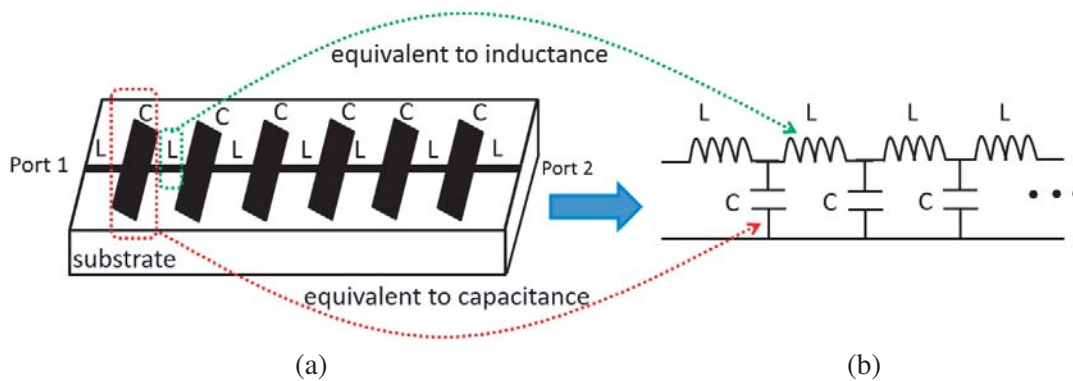
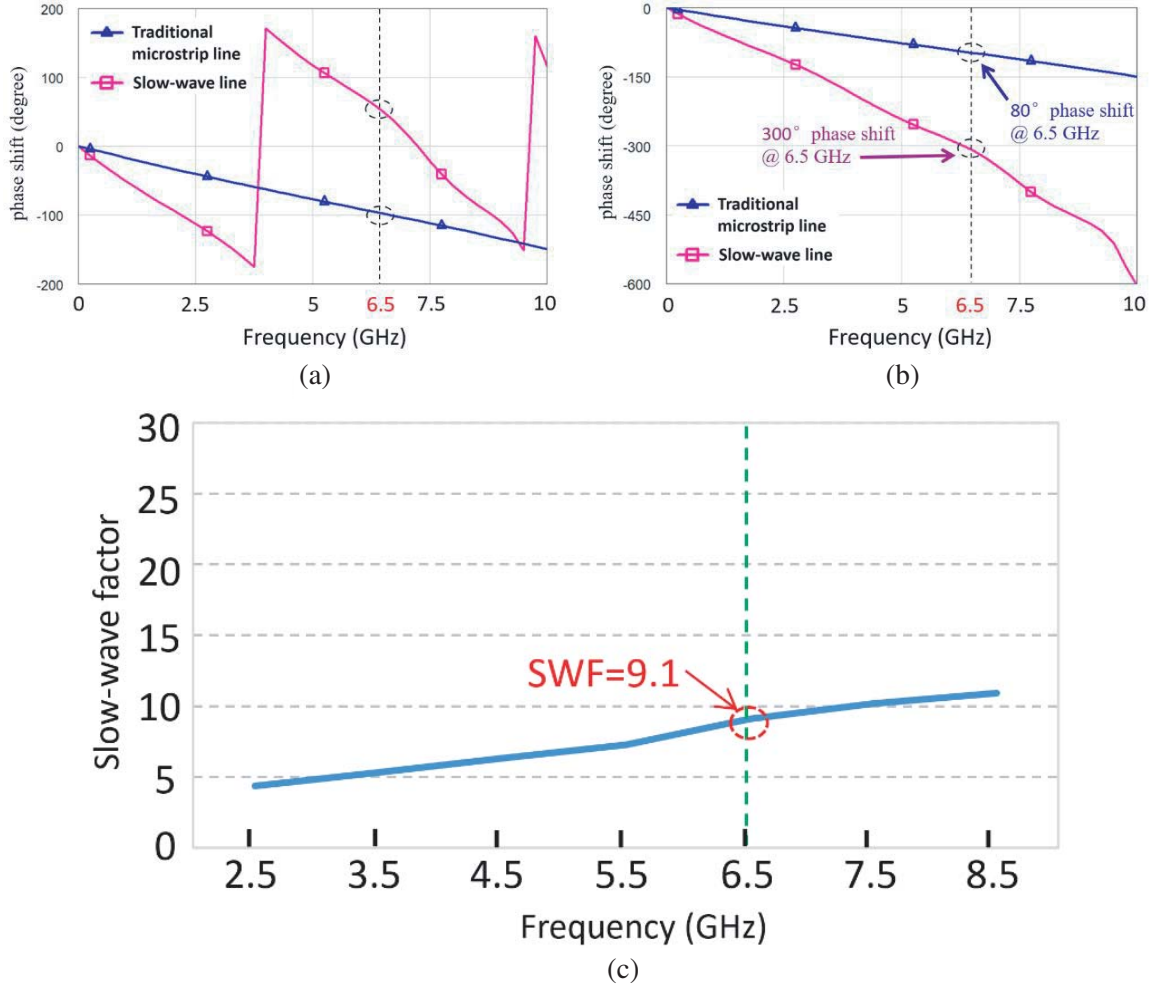


Figure 3. Slow-wave resonator. (a) Structure and (b) its equivalent circuit.

From Eqs. (1)–(3), it follows that the wavelength can be made small while the characteristic impedance is kept unchanged by increasing  $L$  and  $C$  with the same ratio. Figure 4(a) shows the comparison of phase shift between slow-wave line and conventional microstrip line with same physical length. Figure 4(b) is the unwrapped format of Figure 4(a) for a distinct view. The phase shift of the slow-wave line is  $300^\circ$  at 6.5 GHz, whereas phase shift of traditional microstrip line with the



**Figure 4.** Phase shift comparison between slow-wave structure and traditional microstrip line. (a) Wrapped format, (b) unwrapped format and (c) slow-wave factor (SWF).

same physical length resonator is only  $80^\circ$  at 6.5 GHz. The slow-wave line with the same physical length reaches 3.75 times of phase shift compared to that of traditional one, which is great for size reduction. The slow-wave factor (SWF) of the slow-wave resonator reaches 9.1, shown in Figure 4(c). Owing to the usage of slow-wave resonator, the length of each resonator is reduced about 60%. The dielectric constant is 5.9 using Ferro-A6 material, and the thickness of each LTCC layer is 0.1 mm. After an electromagnetic (EM)-optimization, the optimized dimension parameters defined in Figure 1(b) are listed in Table 1. End-coupling capacitances between each pair of adjacent resonators defined in Figure 2 are  $C_{12} = C_{45} = 54$  fF and  $C_{23} = C_{34} = 19$  fF.

**Table 1.** Optimal parameters of the proposed BPF.

Dimensions	$W_1$	$W_2$	$W_3$	$g_1$	$g_2$	$g_3$	$L_1$	$L_2$	$L_3$	$L_4$	$L_5$
Unit (mm)	0.15	0.2	0.24	0.08	0.1	0.18	0.88	0.92	0.98	0.1	0.15



Figure 5. Photograph of the proposed BPF.

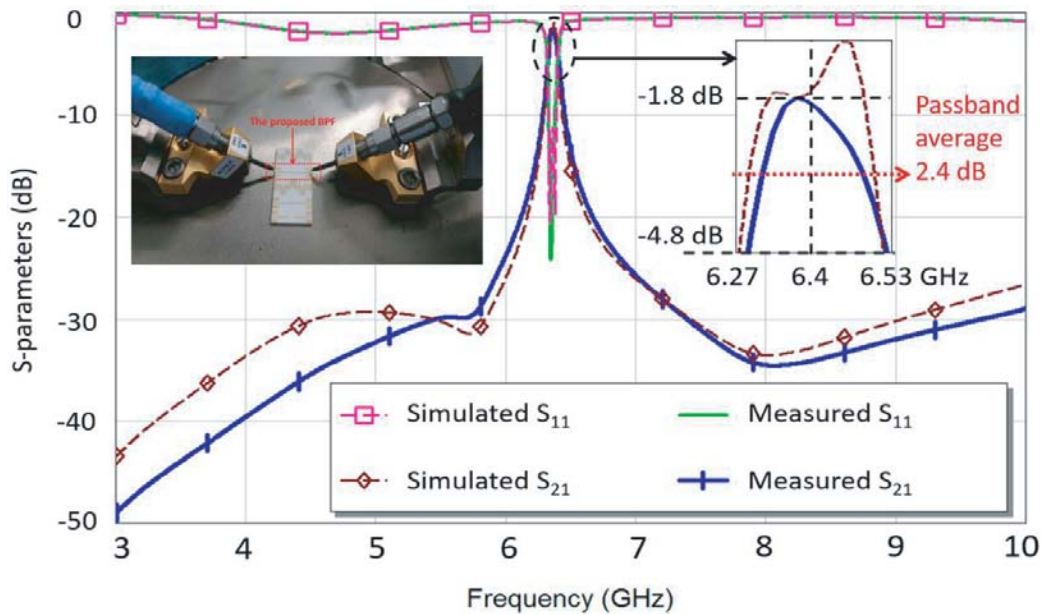


Figure 6. Simulated and measured  $S$ -parameters.

### 3. SIMULATED AND MEASURED RESULTS

Figure 5 shows a photograph of the proposed BPF. The EM-simulation uses AXIEM [15], and measurements are carried out by Agilent N5230C network analyzer and Cascade Microtech Summit 9000 probe station. The simulated and measured results are shown in Figure 6. The center frequency shifts from 6.5 GHz to 6.4 GHz, which is caused by the Ferro-A6 material shrinkage and the surface roughness of top metal. The bandwidth of the proposed BPF is 0.26 GHz (passband from 6.27 to 6.53 GHz), which equals 4% FBW. Measured passband  $S_{21}$  and  $S_{11}$  are better than  $-4.8$  dB and  $-18$  dB, respectively. The average value of passband insertion loss is 2.4 dB. The entire size of the proposed BPF is only  $15 \times 2 \times 0.3$  mm, which achieves a size reduction of 60% by using length-reduced slow-wave resonators compared with traditional planar one.

### 4. DISCUSSION AND COMPARISON

Performances comparisons with other narrowband implementations are listed in Table 2. The implemented BPF has the smallest average passband insertion loss, greatest size reduction, and narrowest FBW among BPFs in [1–12]. Although BPFs in [13, 14] achieved a smaller size and narrower

**Table 2.** Performance and size comparisons.

Ref.	Center frequency (GHz)	FBW	Average passband insertion loss (dB)	Inband return loss (dB)	Topology used	Integration level	Fabrication process
[1]	18	5.50%	5	18	Combine	Low	PCB
[2]	1.62	7.22%	5	15	Split ring resonator	Low	PCB
[3]	0.873	8.60%	2.44	15.5	Split ring resonator	Low	PCB
[4]	2	5%	7.5	10	Resistor-loaded resonator	Low	PCB
[5]	3.5	5.10%	5	15	Cross-coupling	Low	PCB
[6]	34	5.40%	4.1	11	SIW	Medium	PCB
[7]	13.6	4.5%	3.2	15	SIW	Medium	PCB
[8]	1.263	4.1%	3	12	Open-loop resonator	Medium	PCB
[9]	5.8	5%	2.5	15	Right-left hand resonator	Medium	PCB
[10]	60	15%	3	13	End-coupling	High	LTCC
[11]	29.8	4.50%	3	12	End-coupling	High	LTCC
[12]	40	7.14%	3.17	11	End-coupling	High	LTCC
This work	6.5	4%	2.4	18	End-coupling	High	LTCC

FBW, they are not suitable for mass productions because the I/O ports are not on the same side in [13], and extra via transition is needed with a higher passband insertion loss [14].

## 5. CONCLUSION

A miniaturized and narrowband BPF is proposed and fabricated using multilayered LTCC integration technology. Owing to the usage of length-reduced slow-wave resonators and placing adjacent resonator on different layers, 60% size reduction and 4% FBW are achieved. The proposed BPF also solves the problem of minimal gap distance on planar implementation. Performance and size comparisons are implemented as well. The proposed BPF has been equipped on weather detect radar front-end system, and it works very well.

## REFERENCES

1. Alicioğlu, B., G. Boyacıoğlu, S. Oruç, Ç. Yavuz, and N. Yildirim, "A new method for efficient bandwidth control of narrowband planar filters," *Proc. IEEE proceeding European Microwave Conference*, 171–174, 2013.
2. Gholipour, V., R. Hajitashakkori, and A. Alighanbari, "Compact narrowband filter with wide stopband using CSRRs and stub-line loading," *Proc. IEEE 24th Iranian Conference on Electrical Engineering (ICEE)*, 1297–1299, 2016.

3. Wibisono, M. A. and A. Munir, "Utilization of split ring resonator for compact narrowband microstrip bandpass filter," *Proc. IEEE 22nd Asia-Pacific Conference on Communications (APCC)*, 591–594, 2016.
4. Wang, Z., Z. Fu, C. Li, S. Fang, and H. Liu, "A compact negative-group-delay microstrip bandpass filter," *Progress In Electromagnetics Research Letters*, Vol. 90, 45–51, 2020.
5. Yue, Y. and Y. Bo, "Design of cross-coupling ceramic SIR narrowband filter," *IEEE Proceeding on International Conference on Communication Problem-solving*, 29–31, 2014.
6. Shen, M., Z. Shao, X. Li, and Z. He, "Novel multilayered substrate integrated waveguide narrowband filters for millimeter-wave 3D-MCM applications," *Proc. IEEE MTT-S International Wireless Symposium (IWS)*, 1–3, 2016.
7. Hou, W. and Q. Tang, "Linear phase SIW filter with good selectivity," *Progress In Electromagnetics Research Letters*, Vol. 89, 105–111, 2020.
8. Gadhafi, R., D. Cracan, A. A. Mustapha, and M. Sanduleanu, "T-shaped I/O feed based differential bandpass filter with symmetrical transmission zeros and high common mode rejection ratio," *Progress In Electromagnetics Research M*, Vol. 89, 141–149, 2020.
9. Hu, S., Y. Gao, X. Zhang, and B. Zhou, "Design of a compact 5.7–5.9 GHz filter based on CRLH resonator units," *Progress In Electromagnetics Research Letters*, Vol. 89, 141–149, 2020.
10. Hiraga, K., T. Seki, K. Nishikawa, and K. Uehara, "Multi-layer coupled band-pass filter for 60 GHz LTCC system-on-package," *Proc. IEEE Asia-Pacific Conference Proceedings (APMC)*, 259–262, 2010.
11. Choi, B. G., M. G. Stubbs, and C. S. Park, "A Ka-band narrow bandpass filter using LTCC technology," *IEEE Microwave and Wireless Components Letters*, Vol. 13, 388–389, 2003.
12. Ambak, Z., A. Ibrahim, H. M. Hizan, A. I. A. Rahim, M. Z. M. Yusoff, R. Ngah, and Y. C. Lee, "Design of 40 GHz multilayer end coupled band pass filter using LTCC technology," *Proc. IEEE International Conference on Semiconductor Electronics (ICSE)*, 294–297, Kuala Lumpur, Malaysia, 2014.
13. Zhou, B., Q. Wang, P. Ge, Q. Ma, Y. Lu, and C.-H. Cheng, "Compact LTCC filter with end-coupled resonators," *Proc. IEEE International Conference on Electron Devices and Solid-State Circuits (EDSSC) Proceedings*, 1–2, Hsinchu, Taiwan, 2017.
14. Li, Y., "Compact and narrowband LTCC filter using vertically stacked end-coupled resonators," *Microw. Opt. Technol. Lett.*, Vol. 59, 86–89, 2017.
15. AXIEM, Applied Wave Research Corporation, El Segundo, CA, <https://www.awr.com/awr-software/products/axiem>.